Published in final edited form as:
Free Radic Biol Med. 2009 February 15; 46(4): 454–461. doi:10.1016/j.freeradbiomed.2008.10.046.

Immuno-spin-trapping of a post-translational carboxypeptidase B1 radical formed by a dual role of xanthine oxidase and endothelial nitric oxide synthase in acute septic mice

Saurabh Chatterjee[1,*], **Marilyn Ehrenshaft**[1], **Suchandra Bhattacharjee**[1], **Leesa J. Deterding**[2], **Marcelo G. Bonini**[1], **Jean Corbett**[1], **Maria Kadiiska**[1], **Kenneth B Tomer**[2], and **Ronald P Mason**[1]

1 *Free Radical Metabolites Group, Laboratory of Pharmacology, National Institute of Environmental Health Sciences, Research Triangle Park, North Carolina-27709, USA*

2 *Laboratory of Structural Biology, National Institute of Environmental Health Sciences, Research Triangle Park, North Carolina-27709, USA*

Abstract

Post-translational modification of proteins due to exposure to radicals and other reactive species are markers of metabolic and inflammatory oxidative stress such as sepsis. This study uses the nitrone spin-trap DMPO and a combination of immuno-spin trapping and mass spectrometry to identify in vivo products of radical reactions in mice. We report the detection of dose-dependent production of DMPO-carboxypeptidase B1 (CPB1) adducts in the spleen of mice treated with lipopolysaccharide (LPS). Additionally, we report significant detection of DMPO-CPB1 adducts in mice experiencing normal physiological conditions. Treatments with inhibitors and experiments with knock-out mice indicate that xanthine oxidase and endothelial nitric oxide synthase are important sources of the reactive species that lead to CPB1 adduct formation. We also report a significant loss of CPB1 activity following LPS challenge in conjunction with an increase in CPB1 protein accumulation. This suggests the presence of a possible mechanism for CPB1 activity loss with compensatory protein production.

Keywords

oxidative stress; immuno-spin trapping; inflammation; nitrone adduct

Introduction

Free radicals and other reactive oxidant species (ROS) are produced in a wide range of physiological processes[1]. Free radicals and/or ROS have been implicated in systemic inflammatory response syndrome (SIRS), which is typically seen in patients with trauma, asceptic burns, cancer, heatstroke, widespread surgical manipulations and acute pancreatitis. The molecular events and targets of oxidative and nitrosative stress that trigger SIRS are

Correspondence should be addressed to: Dr. Saurabh Chatterjee, PhD., Free Radical Metabolites Group, Laboratory of Pharmacology, National Institute of Environmental Health Sciences, National Institutes of Health, 111 T.W. Alexander Dr., Research Triangle Park, North Carolina 27709,USA. e-mail: chatterjees2@niehs.nih.gov.

unclear, but the clinical and pathological features that typify SIRS mimic that of severe sepsis. The clinical manifestations of sepsis are typically observed in blood-borne infections with Gram-negative bacteria and can be mimicked by administration of lipopolysacharride (LPS), the active component of endotoxin[2–4].

A wide range of complex systems are secondarily stimulated during sepsis, including activation of the complement system comprising the activation products C3a and C5a, platelet-activating factor (PAF), arachidonic acid metabolites, reactive oxygen species (ROS), and nitric oxide (NO). Progression of the disease leads to a vicious cycle of inflammation and coagulation, with ischemia, cell damage, and finally, organ dysfunction and death. There is convincing evidence of severe oxidative stress in patients with sepsis[5]. Because oxygen free radicals and other ROS appear to act as messengers in cellular signal transduction, there are potential implications for a role in the immuno-inflammatory response during sepsis[6]. The increase of ROS after LPS challenge has been demonstrated in different models of septic shock in peritoneal macrophages and lymphocytes[7,8]. This disturbance in the balance between pro-oxidants (ROS) and antioxidants in favor of the former is characteristic of oxidative stress in immune cells in response to endotoxin[7,9].

The observation that reaction of $NO^{\bullet}$ with superoxide ($O_2^{\bullet-}$) yields the reactive species peroxynitrite has increased interest in tyrosyl radical formation and subsequent nitration on enzyme structure-function relationships in diverse clinical pathologies[10–13]. Peroxynitrite not only has novel oxidizing properties but its formation results in decreased bioavailability of NO therefore diminishing its salutary physiological functions. Since the proton-catalyzed homolysis of peroxynitrite is slow relative to second order processes that may occur in vivo, it is evident that peroxynitrite-dependent nitrotyrosine formation in biological systems must be mediated by the previous reaction of peroxynitrite with carbon dioxide or metal centers in order to generate secondary oxidizing species, that in, turn react with tyrosine to form the tyrosyl radical. Thus, in the presence of carbon dioxide, nitration yields increase due to efficient oxidation by the carbonate radical to form tyrosyl radical[14].

Thus, an understanding of the mechanisms underlying protein oxidation and the impact of these post-translational modifications on cell and organ function might provide insight into the pathogenic mechanisms of inflammatory diseases and novel therapeutic strategies for limiting tissue inflammatory injury[15]. The underlying biological effects of free radical formation have been documented as physiological footprints and changes, but literature is scarce for real-time trapping of free radicals in the whole animal. In this work we have utilized the technique of immuno-spintrapping to help elucidate the possible role of oxidative stress, especially arising from peroxynitrite, in sepsis-like syndrome in the whole animal.

To detect protein radicals in systemic inflammation, we administered the nitrone spin trap DMPO to C57BL6/J mice and analyzed proteins from tissue homogenates by immuno-spintrapping and mass spectrometry. We identified a post-translational DMPO-nitrone adduct formed with carboxypeptidase B1 (CPB1) in mice treated with a single bolus dose of LPS. We also discovered lower, but significant, levels of the DMPO-CPB1 adduct in sham-treated mice, indicating that protein radicals form at detectable levels under normal physiological conditions. Experiments with inhibitors and knockout mice were used to determine that xanthine oxidase and endothelial nitric oxide synthase contribute to the formation of CPB1 protein radical. CPB1 is a tissue variety of carboxypeptidase B and is expressed in the pancreas and used as a serum marker for pancreatitis[16]. The results obtained in the course of this study reveal the modulation of CPB1 levels by oxidative microenvironment in spleen in LPS induced systemic inflammation.

Materials and Methods

Materials

LPS (Escherichia coli: Strain 55:B5), CPB from porcine pancreas, 3-morpholinylsydneimine hydrochloride (SIN-1), the xanthine oxidase inhibitor allopurinol and the iNOS inhibitor 1400W [N-(3-(amino methyl)benzyl)acetamide 2HCl] were from Sigma Chemical Co. (St Louis, MO, USA). The spin trap DMPO (5, 5-dimethyl-1-pyrroline N-oxide) was obtained from Alexis Biochemicals, (San Diego, CA, USA). The eNOS inhibitors L-NIO (1-imino-3-butenyl)-L-ornithine, and L-NAME (L-ω-nitroarginine methyl ester) were from Cayman Chemicals, Ann Arbor, MI, USA. (Sigma Chemical Co, USA).

Mice

Adult male, pathogen-free, 8–10 week old C57BL6/J mice (Jackson Laboratories) weighing 23–27 g on arrival were housed for 1 week, one to a cage, before any experimental use. Experiments using mice that contained the disrupted iNOS ($iNOS^{-/-}$), gp91phox ($gp91phox^{-/-}$) and eNOS ($eNOS^{-/-}$) genes were treated identically. Age-matched mice of C57BL6/J origin that had normal iNOS, NADPH oxidase, and eNOS activity served as the control animals for knockout experiments. Mice had ad libitum access to food and water and were housed in a temperature-controlled room at 23–24 °C with a 12-hour light/dark schedule. All animals were treated in strict accordance with the NIH Guide for the Care and Use of Laboratory Animals, and the experiments were approved by the institutional review board.

LPS-induced systemic inflammation model and spin trapping of protein-centered radicals

Mice received a bolus infusion of 6 or 12 mg kg^{-1}LPS at 0 h. Mice screened for protein radical adduct formation also received DMPO, a total of 2 g/kg in two divided doses at +4 and +5 hours post-LPS administration. The sham-treated group received saline in place of LPS and/or DMPO. LPS and DMPO were dissolved in pyrogen-free saline and were administered through the intraperitoneal (i.p.) route. At +6 h, all mice were sacrificed and the spleen and other organs collected and immediately snap-frozen in liquid nitrogen. Tissues were homogenized in phosphate buffer containing 100 μM DTPA and centrifuged at 3,000 RPM at 4 °C for 20 minutes. The samples were stored at −80 °C until further use.

Administration of allopurinol and NOS inhibitors

Allopurinol, a specific inhibitor of xanthine oxidase, the relatively specific eNOS inhibitors (1-imino-3-butenyl)-L-ornithine (L-NIO), 20mg/kg, and L-ω-nitroarginine methyl ester (L-NAME) (Cayman Chemicals, Ann Arbor, MI, USA) and the iNOS inhibitor N-(3-(amino methyl)benzyl) acetamide 2HCl (1400W, Sigma Chemical Co, USA) were all administered i.p. in a single bolus dose of 20 mg/kg 30 minutes prior to LPS treatment.

Mass spectometric analysis for protein identifications

Protein bands manually excised from gels, cut into small pieces, and transferred into a 96-well microtiter plate were subjected to automatic tryptic digestion and analyzed by MALDI/MS and LC/ESI/MS[17]. For all MS analyses, data-dependent acquisitions were acquired in a fully automated mode such that a mass spectrum was acquired followed by MS/MS of the most abundant ions in the spectrum as described in the Supplemental Data. Searches were performed against the NCBI nonredundant protein database using both the MS and the MS/MS data as described in the Supplemental Data.

Immunoprecipitation of DMPO nitrone-adduct and CPB1

Immunoprecipitation of DMPO nitrone adducts was carried out with the Seize X Mammalian immunoprecipitation Kit (Pierce, Rockford, IL, USA) with some modifications. Solubilized

spleen cell homogenates were collected and protein concentrations measured with a Micro BCA Protein Assay Kit (Pierce, Rockford, IL, USA) and adjusted to a concentration of 200 μg/sample. The samples were pre-cleared (1 h at room temperature) with 200 μl of Protein G slurry (50%). The homogenate was incubated overnight with 25 μg of monoclonal antibody to DMPO, and this antigen-antibody mixture was then incubated overnight with the Protein G slurry. Immune complexes were eluted with elution buffer according to the manufacturer's instructions and collected in tubes with 20 μl Tris buffer (pH 9.6). 30 μl of the elution fractions were then resuspended in NuPAGE LDS sample loading buffer with 5 μl of 140 mmol/L 2-mercaptoethanol, heated at 85 °C for 10 minutes and immediately resolved by reducing SDS-PAGE in 4–12% Bis Tris gels (Invitrogen, Carlsbad, CA, USA). CPB1 was immunoprecipitated with polyclonal antibody to CPB1 (R & D Systems, Minneapolis, MN, USA) using the Protein A Immunoprecipitation kit (Pierce, Rockford, IL, USA.) following manufacturer's instructions.

Western Blot Analysis

Following separation by SDS-PAGE, proteins were transferred electrophoretically (40 volts for 40 minutes) to nitrocellulose membranes (Invitrogen, Carlsbad, CA, USA) which were blocked (overnight, 4°C) with 2% Immunoblot blocking reagent (non-fat dry milk) (Upstate Technologies, Temecula, CA, USA) in 0.1M bicarbonate buffer (pH 9.6). For detection of DMPO-nitrone adducts, blots were incubated with rabbit polyclonal antibody to DMPO (1:1000). CPB1 was detected using goat polyclonal antibody to CPB1 (1:1000) (R&D systems, Minneapolis, MN USA). Antibodies specific for xanthine oxidase was purchased from Abcam (Cambridge, MA, USA). After four 10 minute washes in phosphate buffered saline-Tween (PBS-T), the above immunocomplexed membranes were probed (1h at RT) with goat anti-rabbit (1:5000, Upstate Biotechnologies, Temecula, CA, USA), donkey anti-goat (1:3000, R&D Systems, Minneapolis, MN, USA), goat-anti-mouse (1:5000) horseradish peroxidase conjugated secondary antibodies respectively. Probed membranes were washed (10 minutes, PBS-T) four times and immunoreactive proteins were detected using enhanced chemiluminescence (LumiGLO Chemiluminescence Substrate, Upstate, Temecula, CA, USA). The images were subjected to densitometry analysis using LabImage 2006 Professional™ 1D gel analysis software from KAPLEAN Bioimaging Solutions, Germany.

Confocal microscopy of spleen tissue

Mice were administered LPS, Enos inhibitor L-NIO and xanthine oxidase inhibitor allopurinol. DMPO was injected in two divided doses of 1 g/kg at 2h and 1h prior to sacrifice. Spleens were fixed in 10% neutral buffered formalin and soaked in 30% sucrose for 24h. The frozen sections (10 micron) were cryocut using a frozen tissue processor (Leica Instruments, USA) at the immunohistochemistry core facility at NIEHS. Tissue slices were then permeabilised, and blocked (2% nonfat dry milk, Pierce Biomedical, USA). Antibody specific to DMPO nitrone adducts and Alexafluor 488 goat anti-rabbit antibody (Molecular Probes, USA) were used as primary and secondary antibodies, respectively. Confocal images were taken on a Zeiss LSM510-UV meta (Carl Zeiss Inc, Oberkochen, Germany) using a Plan-NeoFluar 40X/1.3 Oil DIC objective. The 488 nm line from an Argon laser was used for producing polarized light for a DIC image as well as fluorescence excitation of the Alexa488 secondary antibody. A longpass 505 emission filter was used to collect the fluorescence images with a pinhole setting of 81 microns. All images were acquired with equal excitation power (5%) and identical detection gain (532 volts).

MetaMorph Offline 7.5.1.0 (Molecular Devices, Downingtown, PA, USA) was used for the calculation of the average fluorescence pixel intensity of the entire image. This data was then entered into Microcal Origin software for statistical analysis

Carboxypeptidase B-like activity assay of CPB1

The mouse carboxypeptidase B1 chromogenic activity assay was carried out using an Actichrome TAFI activity kit (American Diagnostica Inc., Stamford, CT, USA) as per the manufacturer's instructions with some modifications.

Nitric oxide synthase activity assay

Nitric oxide synthase activity in spleen cell homogenates was measured using the colorimetric assay kit from Calbiochem (La Jolla, CA, USA) following the manufacturer's instructions.

Statistical analyses

All in vivo experiments were repeated three times with 3 mice per group. Quantitative data from Western blots as depicted from relative light intensity of the bands were analyzed by performing a one-tailed Student's t test. $P<0.05$ was considered statistically significant.

Results

Detection of CPB1 protein-centered radicals in vivo by immuno-spin trapping

To determine if we could detect LPS-induced DMPO protein adduct formation, mouse tissue homogenates were analyzed using anti-DMPO polyclonal antiserum[17]. While no significant immunoreactivity was detected in liver, lung or kidney tissue, spleen tissue exhibited LPS enhanced production of DMPO protein adducts, and all further analysis was done with spleen. ELISA (Fig. 1A) analysis showed that sham treatment yielded low DMPO immunoreactivity, while LPS treatment produced DMPO protein adducts in a dose-dependent manner. Interestingly, mice treated with DMPO in the absence of LPS (sham + DMPO) produced a statistically significant increase in DMPO adduct formation (Fig. 1A), while LPS treatment yielded a statistically significant increase in DMPO adduct formation over the sham + DMPO treatment.

Western blot analysis corroborated the ELISA data (Fig. 1B). A control Western blot using anti-actin showed that all samples contained comparable amounts of protein. The anti-DMPO Western blot and its corresponding quantification (Fig. 1B) showed a pattern of immunoreactivity identical to the ELISA. We detected statistically significant and dose-dependent increases in DMPO adduct with LPS treatment, but we were also able to detect significant adduct formation in absence of LPS.

Coomassie blue staining (Fig. 1C) showed that LPS treatment produced both qualitative and quantitative changes in extracted proteins, with treated mice accumulating a 62 and 47 kD proteins. However, only the 47 kD protein band corresponded in size to the immunoreactive protein in the anti-DMPO Western blot (Fig 1B). MALDI-TOF analysis of this 47 kD band of resulted in the detection of more than 10 proteins, one of which was carboxypeptidase B1 (CPB1) (data not shown). To increase specificity, we performed two parallel immunoprecipitations of spleen homogenates using 1) anti-DMPO mouse IgG, and 2) goat polyclonal anti-CPB1. A control immunoprecipitation was also performed with normal mouse IgG, and immunoprecipitation products were analyzed by Western blotting using anti-CPB1 (Fig. 2A) and the rabbit polyclonal anti-DMPO (Fig. 2B).

Proteins immunoprecipitated with normal mouse IgG did not contain either detectable CPB1 (Fig. 2A, lane 1) or DMPO adducts (Fig. 2B, lane 1). Proteins immunoprecipitated with either anti-DMPO (Fig. 2A, lane 2) or anti-CBP1 (Fig. 2A, lane 3), however, contained a 47 kD protein that strongly cross-reacted with anti-CBP1 antiserum. This protein also showed strong immunoreactivity when challenged with polyclonal anti-DMPO (Fig. 2B). Further confirmation came from LC/MS/MS analysis of anti-DMPO immunoprecipitation products.

The 47 kD Coomassie blue gel band corresponding to the positive Western band was excised, digested, and analyzed and the protein which scored the highest based on a search of the NCBI non-redundant database was CPB1 (Table 1).

LPS-induced radical formation is mediated by xanthine oxidase

Xanthine oxidase is one of the major endogenous sources of superoxide in the cell and plays a role in superoxide generation in response to LPS in skin tissue[18]. To determine if xanthine oxidase plays a role in either LPS-induced or non-LPS generated CPB1 radical formation, we treated mice with allopurinol, a specific inhibitor of xanthine oxidase. Proteins from spleen tissue homogenates were immunoprecipitated with anti-DMPO and analyzed by Western blotting using anti-CPB1 (Fig. 3, top), and quantification of the resulting blot (Fig. 3, bottom). As seen in Fig. 1, treatment of mice with DMPO allows the unambiguous detection of CPB1 nitrone adduct under endogenous, non-stressed conditions and a further, significant, increase in CPB1-DMPO adduct formation induced by LPS treatment. Administration of allopurinol significantly inhibited adduct formation in both endogenous and LPS-induced adduct formation, indicating a role for xanthine oxidase in both of these processes. To illustrate the immunoreactivity and localization of DMPO nitrone adducts of CPB1 formed due to the administration of LPS in spleen tissue, confocal microscopy was performed. Results indicated that CPB1-DMPO nitrone adducts as exhibited by increased fluorescence, were higher in LPS-treated mice (Fig. 4E) as compared to sham+DMPO treated mice (Fig. 4C). The increase in mean fluroscence intensity was statistically significant as compared to the sham+DMPO treated group (data not shown). LPS administered mice that were treated with allopurinol (Fig. 4G) had significantly reduced mean fluorescent intensity as compared to the LPS - administered group. Also the DMPO nitrone adducts of CPB1 were localized in the sinus lining cells of the red pulp. Western blot analysis of xanthine oxidase levels (Fig. 5) indicated that LPS treatment induced an increased expression that was unaffected by allopurinol.

Endotoxemia modulates carboxypeptidase B-like activity of CPB1

The effect of LPS on CPB1 enzyme function was measured in immunoprecipitated samples using an Actichrome activity kit (Fig. 6). Prior to activity analysis, equal CPB1 protein amounts were verified by ELISA analysis using anti-CPB1 antibody (data not shown). Comparable levels of CPB1 activity were found in all samples from sham-treated mice and were unaffected by the presence of DMPO and/or allopurinol. LPS treatment, however, significantly decreased carboxypeptidase B-like activity compared with the sham treatment group ($p<0.05$). Administration of DMPO to LPS-treated mice alleviated this loss of enzyme activity, while addition of allopurinol alone and allopurinol plus DMPO resulted in increased CPB1 activity ($p<0.01$).

CPB1 radical formation requires endothelial NOS

To determine total NOS activity and the role of specific NOS isozymes in CPB1 protein radical formation, we measured NO levels (as soluble nitrite plus nitrate) in the absence and presence of NOS inhibitors (Fig. 7). LPS induces a significant increase in total NOS activity which is unaffected by 1400W, an inhibitor specific for iNOS. Alternatively, both the general NOS inhibitor, L-NAME, and L-NIO, an eNOS specific inhibitor, decreased levels back to those found in sham-treated mice, indicating that eNOS is essential for the increase in NO in LPS-treated mice.

We then compared CPB1-DMPO adduct levels in wild-type and eNOS knockout mice (Fig. 8). DMPO protein adducts were recovered by immunoprecipitation with anti-DMPO mouse IgG, and CPB1 levels were determined by Western blotting using anti-CPB1. The Western blot itself (Fig. 8, top) clearly shows that eNOS knockout mice contain lower amounts of CPB1-DMPO than wild-type animals, an observation confirmed by quantification of the relative band

intensities (Fig. 8, bottom). Parallel analyses showed that CPB1-DMPO levels were unaltered in either iNOS or gp91phox gene-deficient mice (data not shown).

Influence of LPS on CPB1 protein levels

Membrane-bound B-type carboxypeptidase M (CPM) is upregulated by inflammatory stimuli[19] in human endothelial cells. We used Western blot analysis to determine if LPS treatment had a similar stimulatory effect on spleen CPB1 levels and also to assess if either NOS or xanthine oxidase played a role in this induction (Fig. 9). Anti-actin Western blot analysis showed comparable loading in all lanes (top panel). In comparison, the anti-CPB1 Western blot and its quantification (Fig. 9 middle and bottom panels) clearly show that LPS causes a large increase in spleen CPB1. NOS inhibition had little effect on these levels, but inhibition of xanthine oxidase with allopurinol had a statistically significant effect ($p<0.05$).

Discussion

Generation of free radicals is an early event of inflammation[20], and the original goal of this study was to determine if we could detect protein-radical products of inflammation using antiserum to the spin trap DMPO. Mitochondrial protein radical adducts were detected by immuno-spin trapping in motor neuron degeneration in amyotrophic lateral sclerosis (ALS) [21]. Stadler et al. also showed protein radical formation by immuno-spin trapping in a murine model of acetone-induced ketosis[22]. We chose to extend the studies in an LPS- induced sepsis model to further characterize and identify proteins that formed DMPO nitrone adducts in vivo with immunological techniques and mass spectrometry. We focused on spleen tissue from LPS-treated mice and determined that we could detect a LPS dose-dependent increase in DMPO protein adducts (Fig. 1A and B) with no detectable DMPO-trappable radical formation in liver with immuno-spintrapping at 6h. In the course of these same experiments we also discovered our detection method was sensitive enough to detect DMPO-protein adduct formation in non-treated animals. Therefore, the results obtained in this study not only confirm but also identify for the first time protein radicals generated by LPS- induced oxidative stress and present in normal physiological conditions. Despite limited reports of ROS generation in normal physiology[23,24], we detected substantial in vivo DMPO-trapping of protein free radicals under normal physiological conditions. Not surprisingly, LPS-induced systemic inflammation in mice produced even higher levels of DMPO-protein adducts.

A combination of approaches allowed us to ascertain that CPB1 was adducted to DMPO. Mass spectrometry suggested that the 47 kD immunoreactive band detected in Fig. 1 could be CPB1. Parallel immunoprecipitation experiments using anti-CPB1 and anti-DMPO in conjunction with Western blotting showed that the protein band with immunoreactivity to both CPB1 and DMPO co-immunoprecipitated (Fig. 2). LC/MS/MS examination of the 47 kD immunoreactive band from the anti-DMPO immunoprecipitation experiment identified CPB1 as the most likely protein present (Table 1).

There are a number of potential radical sources in LPS-treated mice, including superoxide anion formation from xanthine oxidase and/or NADPH oxidases[25]. Xanthine oxidase has a principal role in the formation of lipid-derived free radicals in LPS-induced skin inflammation[18] and is upregulated in the spleen in mice suffering cecal ligation and puncture-induced sepsis[26]. In addition, LPS-induced inflammatory events are mediated by the robust upregulation of NADPH oxidases and the phosphorylation of $p47^{phox}$ [27].

While NADPH oxidase knockout mice (gp91phox) did not have reduced levels of CPB1-DMPO (data not shown), the role of xanthine oxidase is clearly substantial. LPS treatment resulted in increased amounts of xanthine oxidase (Fig. 5) in agreement with Chinnaiyan et al[26] who reported the upregulation of xanthine oxidase gene expression in the septic spleen.

Though xanthine oxidase concentrations are higher in liver, the absence of detectable DMPO-trapped radical adducts at 6h might be related to the existence of a coordinated anti-oxidant defense system. This consists of higher glutathione pools and higher expression of SOD, glutathione peroxidase and catalase in the hepatic sinusoidal cells (28,29,30). Additionally, inhibition of xanthine oxidase with allopurinol[31] reduced the amounts of CPB1-DMPO detected in unstressed mice by about 50% and reduced the amount of CPB1-DMPO in LPS treated mice (Fig. 3, Fig. 4G) by greater than 90%. Both of these reductions were due to inhibition of enzyme activity rather than enzyme levels (Fig. 5), indicating that the superoxide production catalyzed by xanthine oxidase production plays an important role in the formation of CPB1 radicals in unstressed tissue and a dominant role in LPS-treated tissue.

The majority of deaths among critically ill patients requiring intensive care are attributable to sepsis and its sequelae; septic shock, SIRS and acute respiratory distress syndrome (ARDS). Experimental and clinical evidence demonstrates that these patients suffer from severe oxidative stress-mediated tissue injury[32]. Among the principle oxidants associated with this pathophysiology is peroxynitrite, a reactive and short-lived species that promotes oxidative damage at the molecular and tissue level in various diseases including diabetes[13,33] Neuronal and endothelial NOS constitutively mediate NO levels but are increasingly seen as prominent players in inflammation, with endothelial-derived NOS recognized as a marker for initial hypotensive events during early sepsis[34–35]. While iNOS is believed to play a prominent role under inflammatory conditions, this study shows that specific inhibition of iNOS did not prevent NOS level increases due to LPS treatment at 6h. Inhibition of eNOS, however, using either the general inhibitor L-NAME or the more specific inhibitor L-NIO did reduce NOS levels to that found in the sham controls (Fig. 6).

Experiments with knock-out mice corroborated the NOS measurements. Mice deficient in iNOS produced the same level of CPB1-DMPO adducts as wild-type mice (data not shown). CPB1-DMPO adduct levels in eNOS knockout mice were decreased about 50%, indicating at least a contributory role for eNOS in production of LPS-induced protein radicals. Recent studies in our laboratory by Bonini et al.[36] emphasized that caution must be maintained while interpreting results from experiments with eNOS knock-out mice as these mice can show compensatory nNOS activity. The residual DMPO adduct formation in eNOS gene-deficient mice might be as a result of increased nNOS activity.

Our results clearly show a significant increase in the levels of nitric oxide in LPS-treated mice (Fig. 7) concomitant with increased protein radical adduct formation (Fig. 1). Increased nitric oxide production (Fig. 7) in conjunction with increased levels of xanthine oxidase (Fig. 5) could lead to peroxynitrite formation, suggesting a potential mechanism for CPB1 radical formation. Peroxynitrite can inhibit Cu, Zn and Mn superoxide dismutase enzymes, glutathione reductase and several other enzymes[37,38]. LPS-treatment results in production of CPB1 protein radicals and also causes both a notable decrease in enzyme activity (Fig. 6) and an increase in CPB1 protein levels. Inhibition of xanthine oxidase by allopurinol suppresses protein radical production (Fig. 3, Fig. 4G), alleviates the reduction of enzyme activity (fig. 6) and also attenuates the increase in protein levels in response to LPS (Fig. 9). These data suggest there might be a possible mechanism for both detecting damaged CPB1 and also for compensating for the loss of CPB1 activity by increased protein accumulation. Thus, the oxidative microenvironment appears to play an important role in regulation of CPB1 expression during inflammation.

Though plasma carboxypeptidase B, also called thrombin activatable fibrinolysin inhibitor (TAFI) or CPB2, has been extensively studied for its regulatory role in inflammation, much less is known about CPB1. CPB1 is the more stable tissue isoform of the carboxypeptidase B family and is found in elevated levels in acute pancreatitis[16,39]. Metallocarboxypeptidases

(MCPs), especially those which belong to the carboxypeptidase B subfamily, are known to regulate inflammation[39,40]. In conclusion, our results suggest an outline for a specific post-translational event involving the formation of CPB1 radical in the murine model of systemic inflammation. Radical formation mediated by eNOS and xanthine oxidase contribute NO and superoxide anion, resulting in peroxynitrite formation. Peroxynitrite decomposition into carbonate and nitrogen dioxide radicals may produce CPB1 radicals, trappable by DMPO (Scheme 1). This report highlights the significance of a broader role of CPB1 in sepsis as is evidenced by increased levels of this enzyme in LPS-treated groups. This report also emphasizes the role of CPB1 radical formation as an early biomarker in systemic inflammation. Finally we report the detection of CPB1protein radical from non-stressed animals undergoing normal metabolic processes.

Acknowledgements

This work has been supported by the Intramural Research Program of the National Institutes of Health and the National Institute of Environmental Health Sciences. The authors sincerely acknowledge Dario C. Ramirez, T. Balkrishna Poduval and Jason Williams for their valuable input and suggestions. We sincerely thank Krisztian Stadler for valuable suggestions on immunostaining for confocal microscopy and Jeff Tucker for image analysis. We also sincerely thank Mary Mason and Ann Motten for helping in careful editing of this manuscript.

Abbreviations

NOS
: nitric oxide synthase

LC/MS
: Liquid chromatography/ Mass Spectrometry

SDS-PAGE
: Sodium dodecyl sulphate – Polyacrylamide gel electrophoresis

References

1. Winterbourn CC. Reconciling the chemistry and biology of reactive oxygen species. Nat Chem Biol 2008;4:278–286. [PubMed: 18421291]
2. Beutler B. Sepsis begins at the interface of pathogen and host. Biochem Soc Trans 2001;29:853–859. [PubMed: 11709087]
3. Beutler B, Du X, Poltorak A. Identification of Toll-like receptor 4 (Tlr4) as the sole conduit for LPS signal transduction: genetic and evolutionary studies. J Endotoxin Res 2001;7:277–280. [PubMed: 11717581]
4. Johnson GB, Brunn GJ, Platt JL. Cutting edge: an endogenous pathway to systemic inflammatory response syndrome (SIRS)-like reactions through Toll-like receptor 4. J Immunol 2004;172:20–24. [PubMed: 14688304]
5. Guo RF, Ward PA. Role of oxidants in lung injury during sepsis Antioxid. Redox Sign 2007;9:991–2002.
6. Victor VM, Rocha M, Esplugues JV, De la Fuente M. Role of free radicals in sepsis: antioxidant therapy. Curr Pharm Design 2005;11:3141–3158.
7. Victor VM, De la Fuente M. Immune cells redox state from mice with endotoxin-induced oxidative stress. Involvement of NF-kB. Free Radic Res 2003;37:19–27. [PubMed: 12653213]
8. DeLeo FR, et al. Neutrophils exposed to bacterial lipopolysaccharide upregulate NADPH oxidase assembly. J Clin Invest 1998;101:455–463. [PubMed: 9435318]
9. Victor VM, et al. Effects of endotoxic shock in several functions of murine peritoneal macrophages. Mol Cell Biochem 1998;189:25–31. [PubMed: 9879650]

10. Beckman JS, Beckman TW, Chen J, Marshall PA, Freeman BA. Apparent hydroxyl radical production by peroxynitrite: implications for endothelial injury from nitric oxide and superoxide. Proc Natl Acad Sci USA 1990;87:1620–1624. [PubMed: 2154753]
11. Augusto O, Bonini MG, Trindade D. Spin trapping of glutathiyl and protein radicals produced from nitric oxide-derived oxidants. Free Radic Biol Med 2004;36:1224–1232. [PubMed: 15110387]
12. Bonini MG, Radi R, Ferrer-Sueta G, Ferreira AM, Augusto O. Direct EPR detection of the carbonate radical anion produced from peroxynitrite and carbon dioxide. J Biol Chem 1999;274:10802–10806. [PubMed: 10196155]
13. Radi R, Peluffo G, Alvarez MN, Naviliat M, Cayota A. Unraveling peroxynitrite formation in biological systems. Free Radic Biol Med 2001;30:463–488. [PubMed: 11182518]
14. Alvarez B, Radi R. Peroxynitrite reactivity with amino acids and proteins. Amino Acids 2003;25:295–311. [PubMed: 14661092]
15. Schopfer FJ, Baker PR, Freeman BA. NO-dependent protein nitration: a cell signaling event or an oxidative inflammatory response? Trends Biochem Sci 2003;28:646–654. [PubMed: 14659696]
16. Kalinina E, et al. A novel subfamily of mouse cytosolic carboxypeptidases. FASEB J 2007;21:836–850. [PubMed: 17244818]
17. Detweiler CD, et al. Immunological identification of the heart myoglobin radical formed by hydrogen peroxide. Free Radic Biol Med 2002;33:364–369. [PubMed: 12126758]
18. Nakai K, Kadiiska MB, Jiang JJ, Stadler K, Mason RP. Free radical production requires both inducible nitric oxide synthase and xanthine oxidase in LPS treated skin. Proc Nat Acad Sci, USA 2006;103:4616–4621. [PubMed: 16537416]
19. Sangsree S, Brovkovych V, Minshall RD, Skidgel RA. Kininase I-type carboxypeptidases enhance nitric oxide production in endothelial cells by generating bradykinin B1 receptor agonists. Am J Physiol Heart Circ Physiol 2003;284:H1959–H1968. [PubMed: 12623793]
20. Sato K, et al. In vivo lipid-derived free radical formation by NADPH oxidase in acute lung injury induced by lipopolysaccharide: a model for ARDS. FASEB J 2002;16:1713–1720. [PubMed: 12409313]
21. Cassina P, et al. Mitochondrial dysfunction in SOD1G93A-bearing astrocytes promotes motor neuron degeneration: prevention by mitochondrial-targeted antioxidants. J Neurosci 2008;28:4115–4122. [PubMed: 18417691]
22. Stadler K, Bonini MG, Dallas S, Duma D, Mason RP, Kadiiska MB. Direct evidence of iNOS-mediated in vivo free radical production and protein oxidation in acetone-induced ketosis. Am J Physiol Endocrinol Metab 2008;295:E456–E462. [PubMed: 18559982]
23. Williams MD, Leigh JS, Chance B. Hydrogen peroxide in human breath and its probable role in spontaneous breath luminescence. Ann N Y Acad Sci 1982;386:478–483.
24. Boveris A, Chance B. Mitochondrial generation of hydrogen peroxide-general properties and effect of hyperbaric oxygen. Biochem J 1973;134:707–716. [PubMed: 4749271]
25. Salvemini D, Doyle TM, Cuzzocrea S. Superoxide, peroxynitrite and oxidative/nitrative stress in inflammation. Biochem Soc Trans 2006;34:965–970. [PubMed: 17052238]
26. Chinnaiyan AM, et al. Molecular signatures of sepsis: multiorgan gene expression profiles of systemic inflammation. Am J Pathol 2001;159:1199–1209. [PubMed: 11583946]
27. Wu F, Schuster DP, Tyml K, Wilson JX. Ascorbate inhibits NADPH oxidase subunit p47phox expression in microvascular endothelial cells. Free Radic Biol Med 2007;42:24–31.
28. Spolarics Z, Stein DS, Garcia ZC. Endotoxin stimulates hydrogen peroxide detoxifying activity in rat hepatic endothelial cells. Hepatology 1996;24:691–692. [PubMed: 8781344]
29. Spolarics Z, Wu JX. Role of glutathione and catalase in H2O2 detoxification in LPS-activated hepatic endothelial and Kupffer cells. Am J Physiol 1997;273:G1304–1311. [PubMed: 9435555]
30. Spolarics Z. Endotoxemia, pentose cycle, and the oxidant/antioxidant balance in the hepatic sinusoid. J Leukoc Biol 1998;63:534–541. [PubMed: 9581796]
31. Pacher P, Nivorozhkin A, Szabó C. Therapeutic effects of xanthine oxidase inhibitors: renaissance half a century after the discovery of allopurinol. Pharmacol Rev 2006;58:87–114. [PubMed: 16507884]

32. Gutteridge JMC, Mitchell J. Redox imbalance in the critically ill. Br Med Bull 1999;55:49–55. [PubMed: 10695079]

33. Stadler K, Bonini MG, Dallas S, Jiang J, Radi R, Mason RP, Kadiiska MB. Involvement of inducible nitric oxide synthase in hydroxyl radical-mediated lipid peroxidation in streptozotocin-induced diabetes. Free Radical Biol Med 2008;45:866–874. [PubMed: 18620046]

34. Yang CS, et al. Roles of peroxiredoxin II in the regulation of proinflammatory responses to LPS and protection against endotoxin–induced lethal shock. J Exp Med 2007;204:583–594. [PubMed: 17325201]

35. Connelly L, Madhani M, Hobbs AJ. Resistance to endotoxic shock in endothelial nitric-oxide synthase (eNOS) knock-out mice: a pro-inflammatory role for eNOS-derived no in vivo. J Biol Chem 2005;280:10040–10046. [PubMed: 15647265]

36. Bonini MG. Constitutive nitric oxide synthase activation is a significant route for nitroglycerine-mediated vasodilation. Proc Natl Acad Sci USA 2008;105:8569–8574. [PubMed: 18562300]

37. MacMillan-Crow LA, Crow JP, Thomson JA. Peroxynitrite-mediated inactivation of manganese superoxide dismutase involves nitration and oxidation of critical tyrosine residues. Biochemistry 1998;37:1613–1622. [PubMed: 9484232]

38. Alvarez B, et al. Inactivation of human Cu, Zn superoxide dismutase by peroxynitrite and formation of histidinyl radical. Free Radic Biol Med 2004;37:813–822. [PubMed: 15304256]

39. Hilal MA, Ung CT, Westlake S, Johnson CD. Carboxypeptidase-B activation peptide, a marker of pancreatic acinar injury, but not L-selectin, a marker of neutrophil activation, predicts severity of acute pancreatitis. J Gastroenterol Hepatol 2007;22:349–354. [PubMed: 17295766]

40. Arolas JL, Vendrell J, Aviles FX, Fricker LD. Metallocarboxypeptidases: emerging drug targets in biomedicine. Curr Pharm Design 2007;13:347–364.

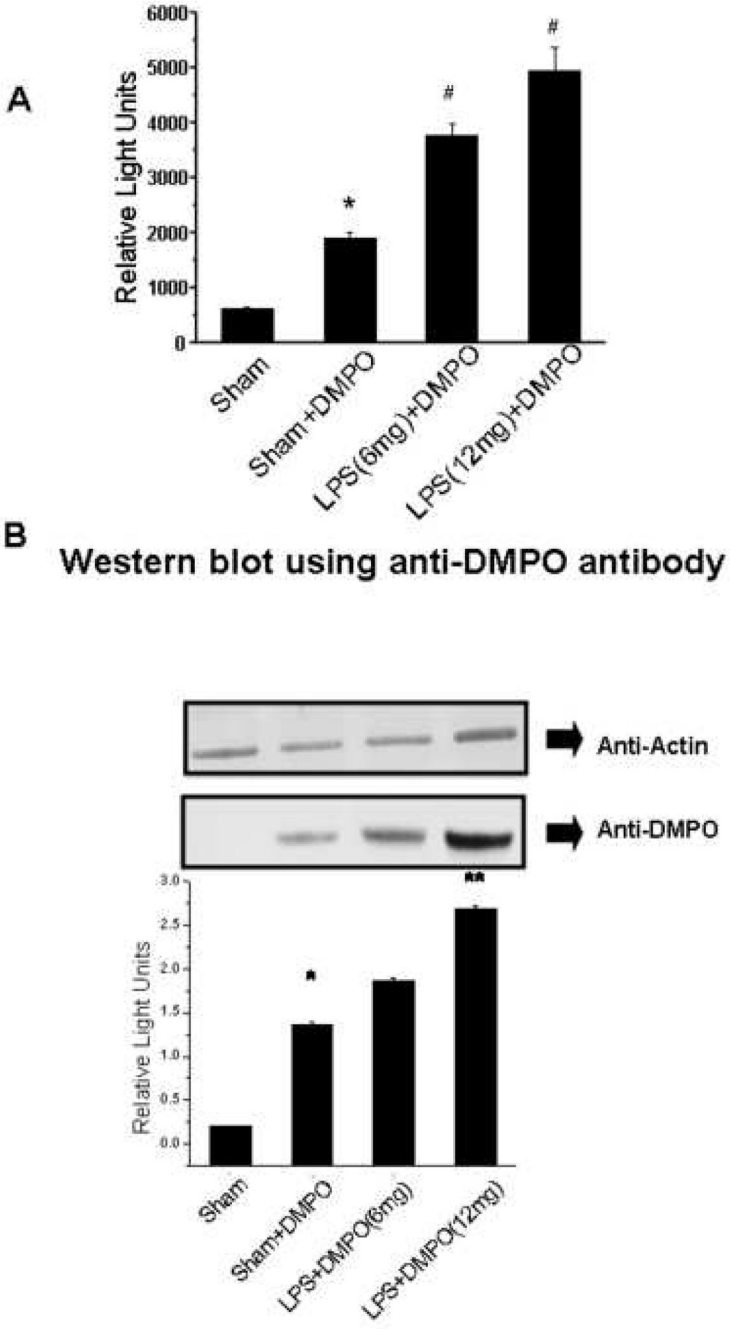

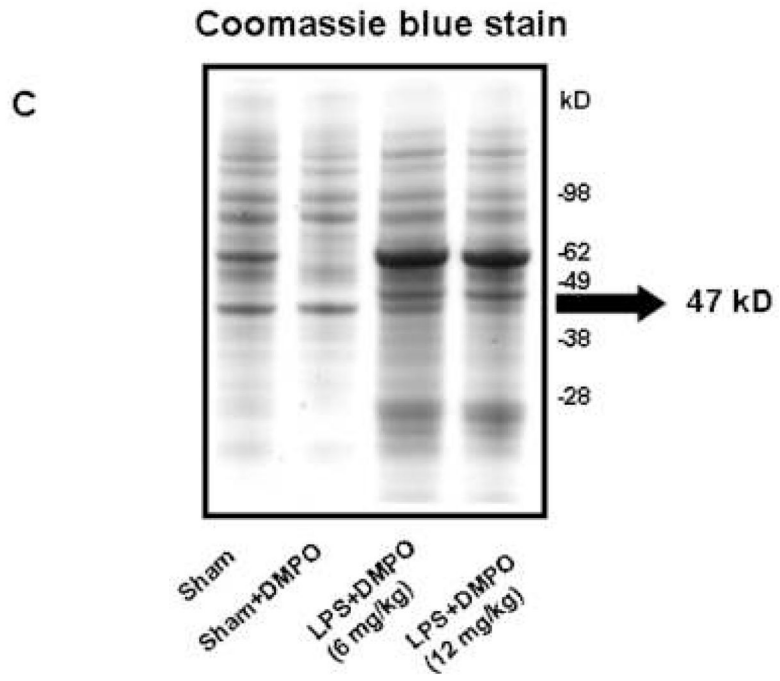

Fig. 1. Immunological detection of DMPO-protein adducts in spleen tissue homogenates

Spleen tissue homogenates from mice treated as described in the materials and methods were examined by immunological methods and Coomassie blue staining. **A)** ELISA analysis using anti-DMPO polyclonal rabbit antiserum showing values significantly different ($P<0.05$) from the sham sample indicated by an asterisk (*) and values significantly different ($P<0.05$) from the sham+DMPO sample indicated by a #. **B)** Representative Western blots analyzed with anti-actin antibody (top panel) as a loading control and anti-DMPO antibody (middle-panel). The bottom panel shows the relative band intensity of the data from the anti-DMPO Western blot. Values represent the mean ± SE, with values significantly different ($P<0.05$) from the sham sample indicated by an asterisk (*) and values significantly different ($P<0.05$) from the sham + DMPO sample indicated by #. **C)** Coomassie blue-stained gel indicating a 47 kD band used for MALDI-TOF.

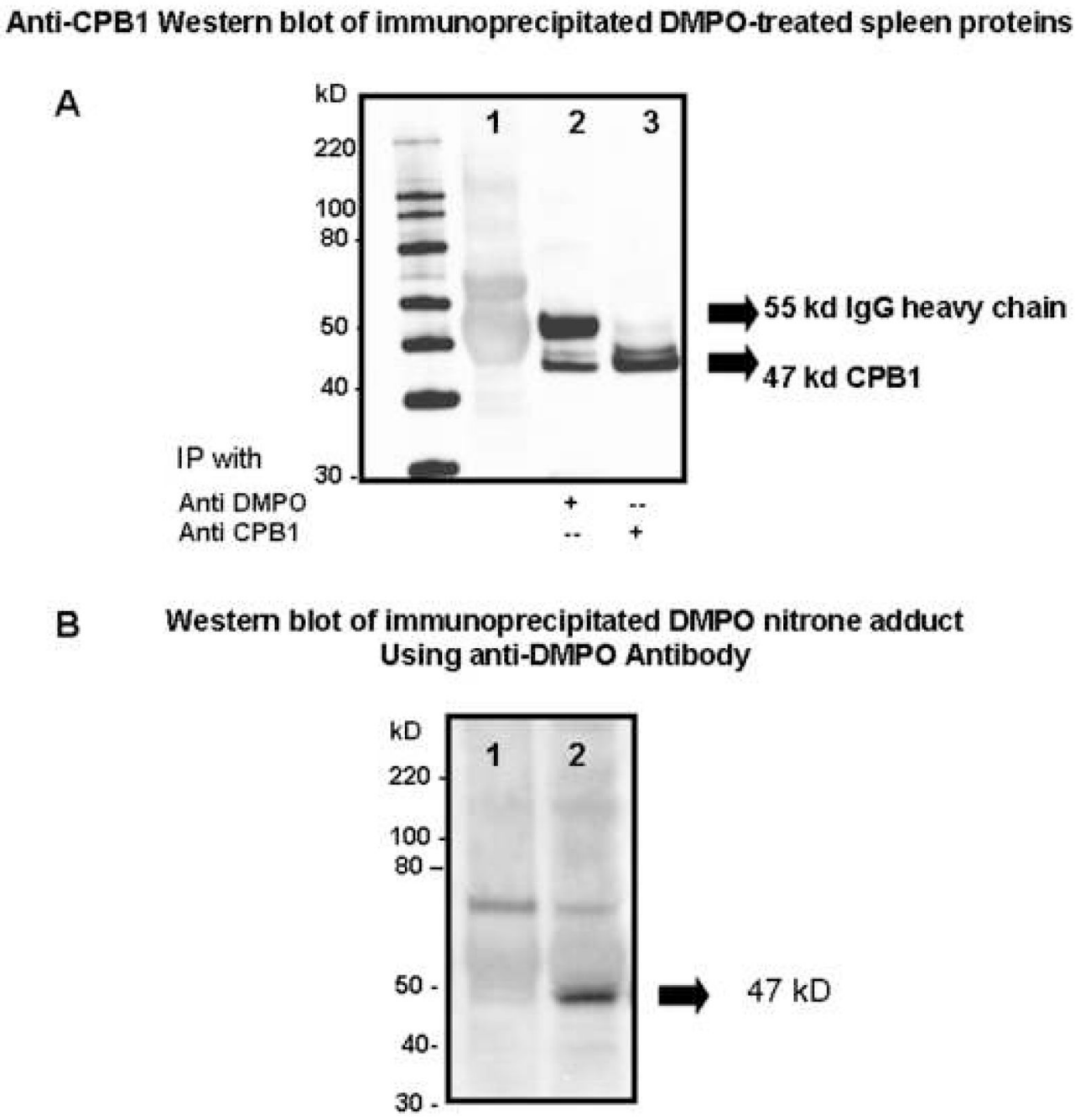

Fig. 2. Immunoprecipitation of DMPO-adducts

Proteins were immunoprecipitated from spleen tissue homogenates using either normal mouse IgG as a control or with anti-DMPO mouse IgG or goat anti-CPB1. **A)** Western blot analysis of immunoprecipitates using goat anti-CPB1. Lane 1, normal mouse IgG; lane 2, anti-DMPO mouse IgG; lane 3, goat anti-CPB1. **B)** Western analysis of immunoprecipitates using rabbit polyclonal anti-DMPO. Lane 1, normal mouse IgG; lane 2, anti-DMPO mouse IgG. Blots are representative of 3 different immunoblots from an equal number of experiments.

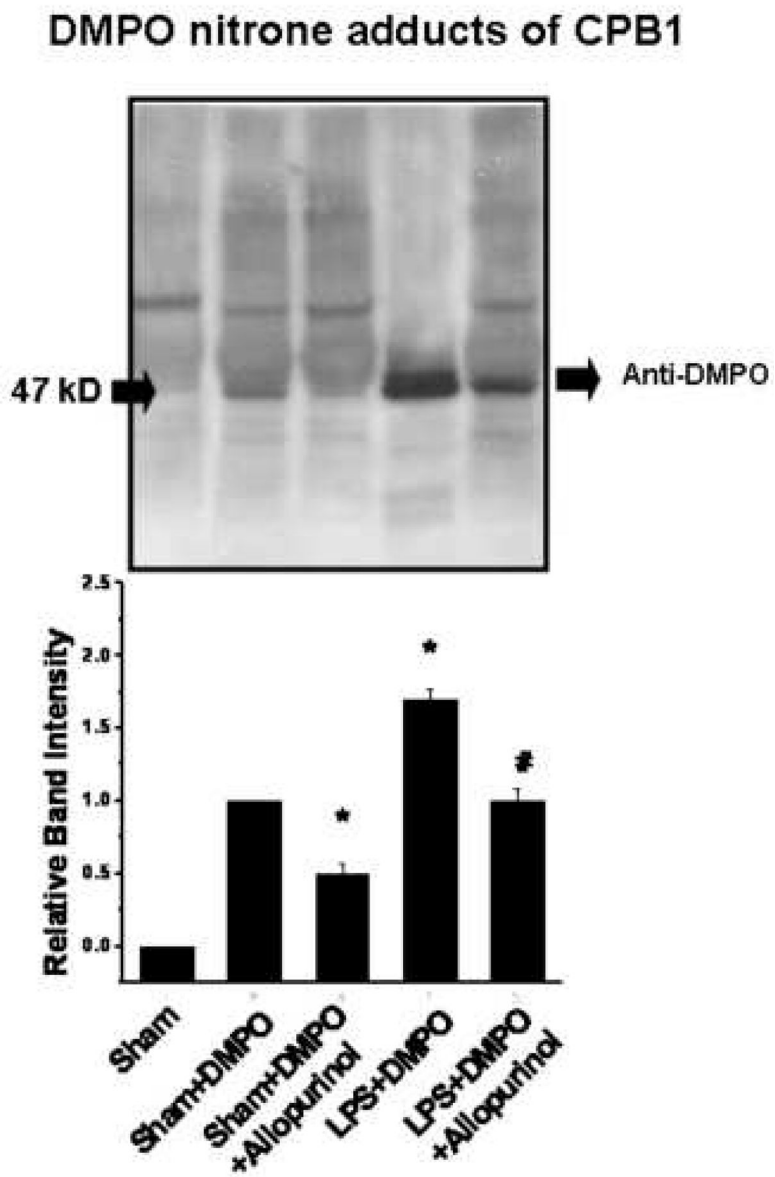

Fig. 3. Effect of allopurinol inhibition of xanthine oxidase on CPB1-DMPO adduct formation

Protein from spleen tissue homogenates from mice treated as shown were immunoprecipitated using anti-DMPO and were analyzed by Western blotting using anti-CPB1 (top panel). The Western blot represents results from 3 independent experiments with the best figure being displayed. Relative band intensities from the scanned Western blot are shown in the bottom panel. Values significantly different ($P<0.05$) from the sham+DMPO sample are indicated by an asterisk (*) while values significantly different ($P<0.05$) from the LPS+DMPO sample are indicated by #.

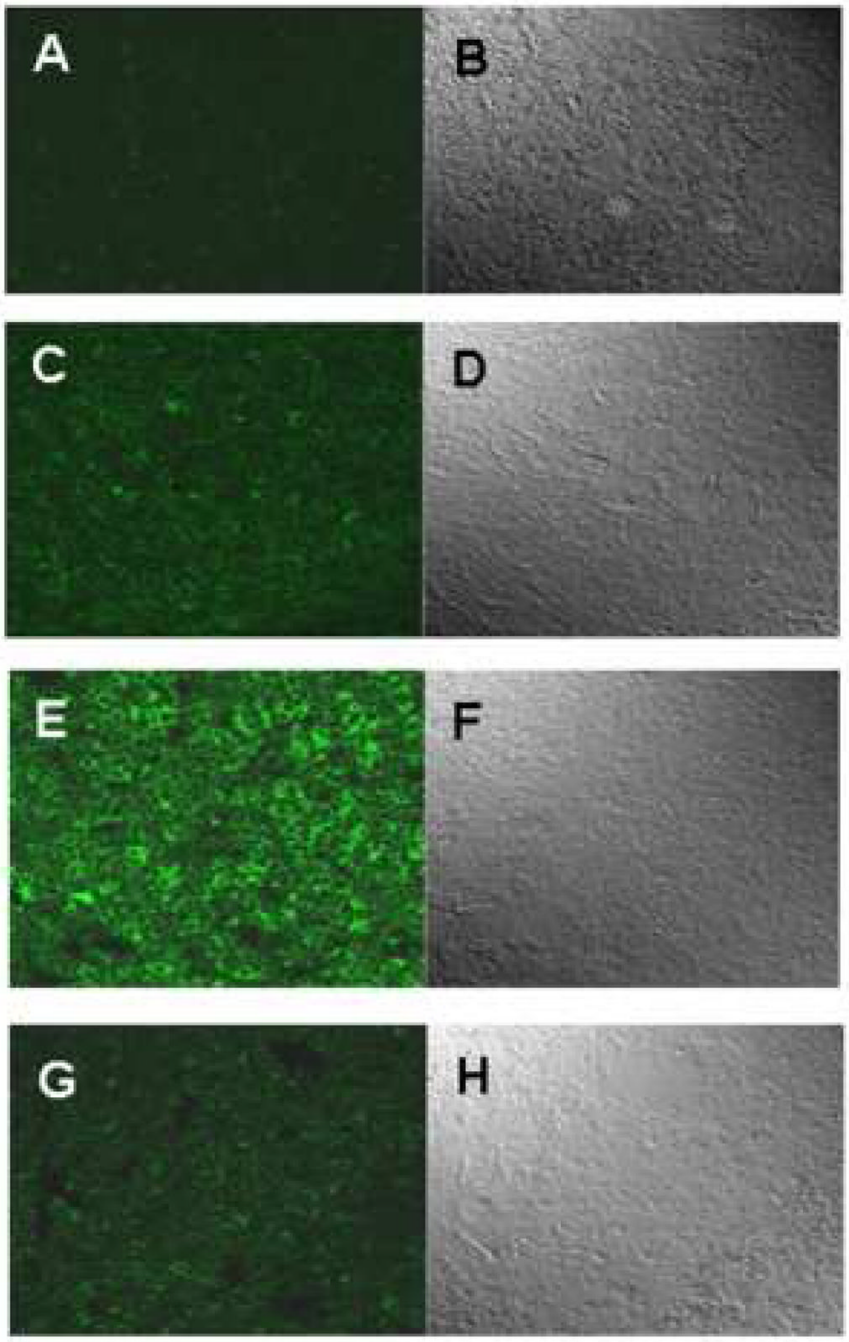

Fig. 4. Confocal microscopy of spleen tissue

Mice were administered LPS, eNOS inhibitor L-NIO and xanthine oxidase inhibitor allopurinol. DMPO was injected in two divided doses of 1 g/kg at 2h and 1h prior to sacrifice. Spleens were fixed in 10% neutral buffered formalin, and then the frozen sections (10 micron) were cryocut. Tissue slices were then permeabilised, blocked (2% nonfat dry milk, Pierce Biomedical, USA). Antibody specific to DMPO nitrone adducts and Alexafluor 488 goat anti rabbit were used as primary and secondary antibodies, respectively. A, C, E and G represent images from sham, sham+DMPO, LPS and LPS+allopurinol, respectively. Images on the right panel (B, D, F and H) represent the corresponding differential interference contrast (DIC) images.

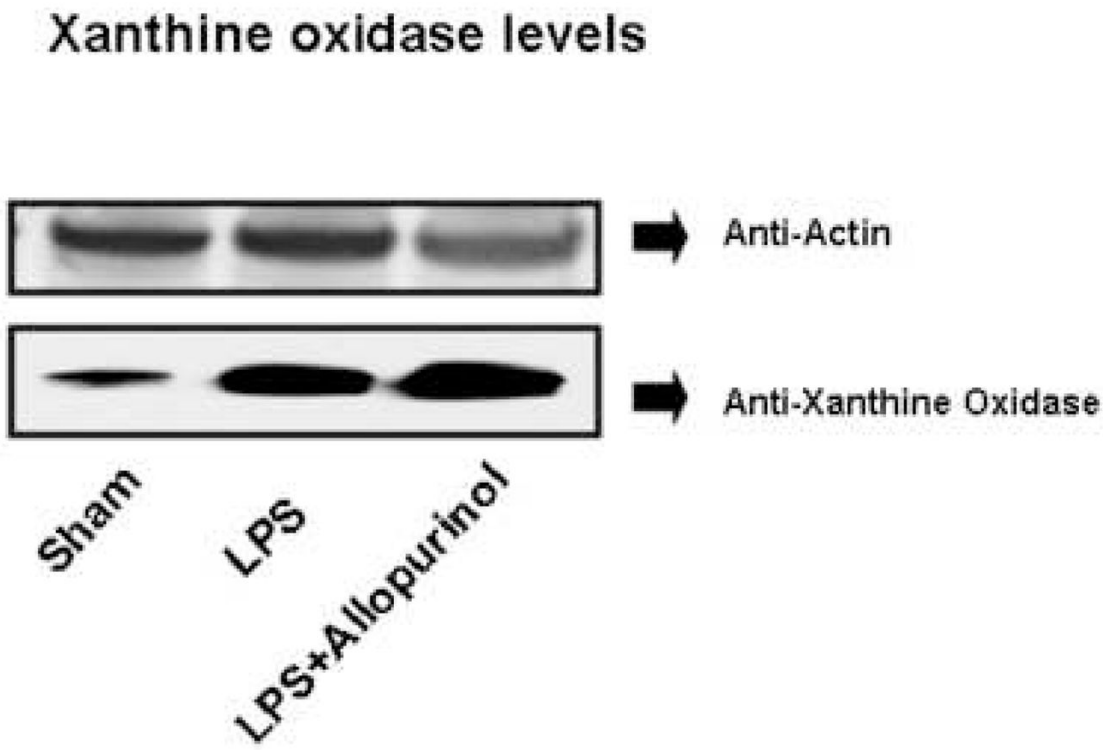

Fig. 5. Xanthine oxidase levels

Protein from spleen tissue homogenates from mice treated as shown was analyzed by Western blotting using anti-actin (top panel) and anti-xanthine oxidase antibodies.

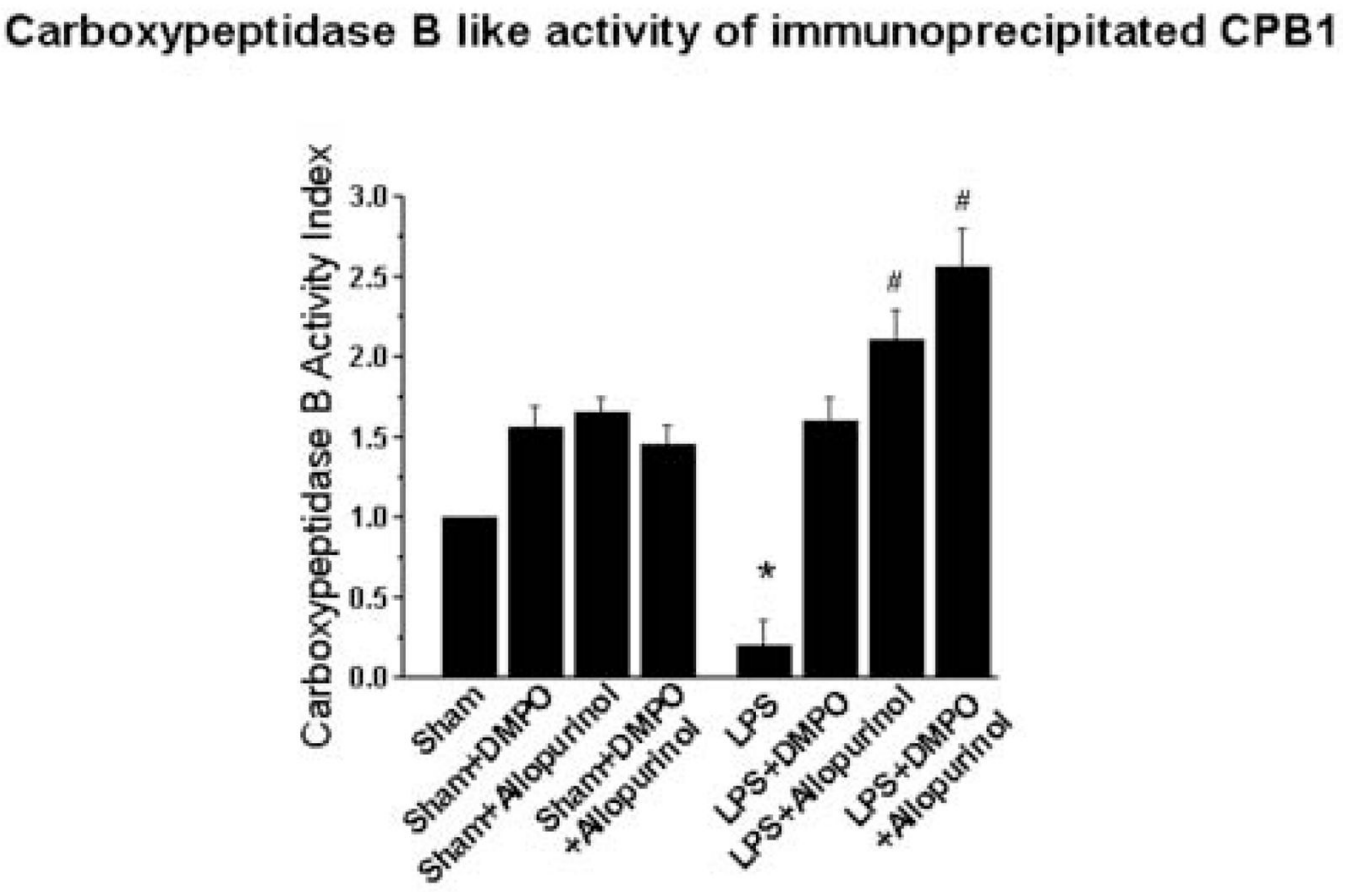

Fig. 6. Carboxypeptidase B-like activity

Anti-CPB1 was used to immunoprecipitate protein from spleen tissue homogenates from mice treated as shown, and CPB1 levels were determined to be equal by western analysis (data not shown). Carboxypeptidase B like activity was determined as described in the materials and methods. Data shown are the mean ± SE of CPB-like activity compared to the activity from sham-treated samples (defined as equal to 1). Values significantly different ($P<0.05$) from the sham sample are indicated by an asterisk (*), while values significantly different ($P<0.01$) from the LPS sample are indicated by #.

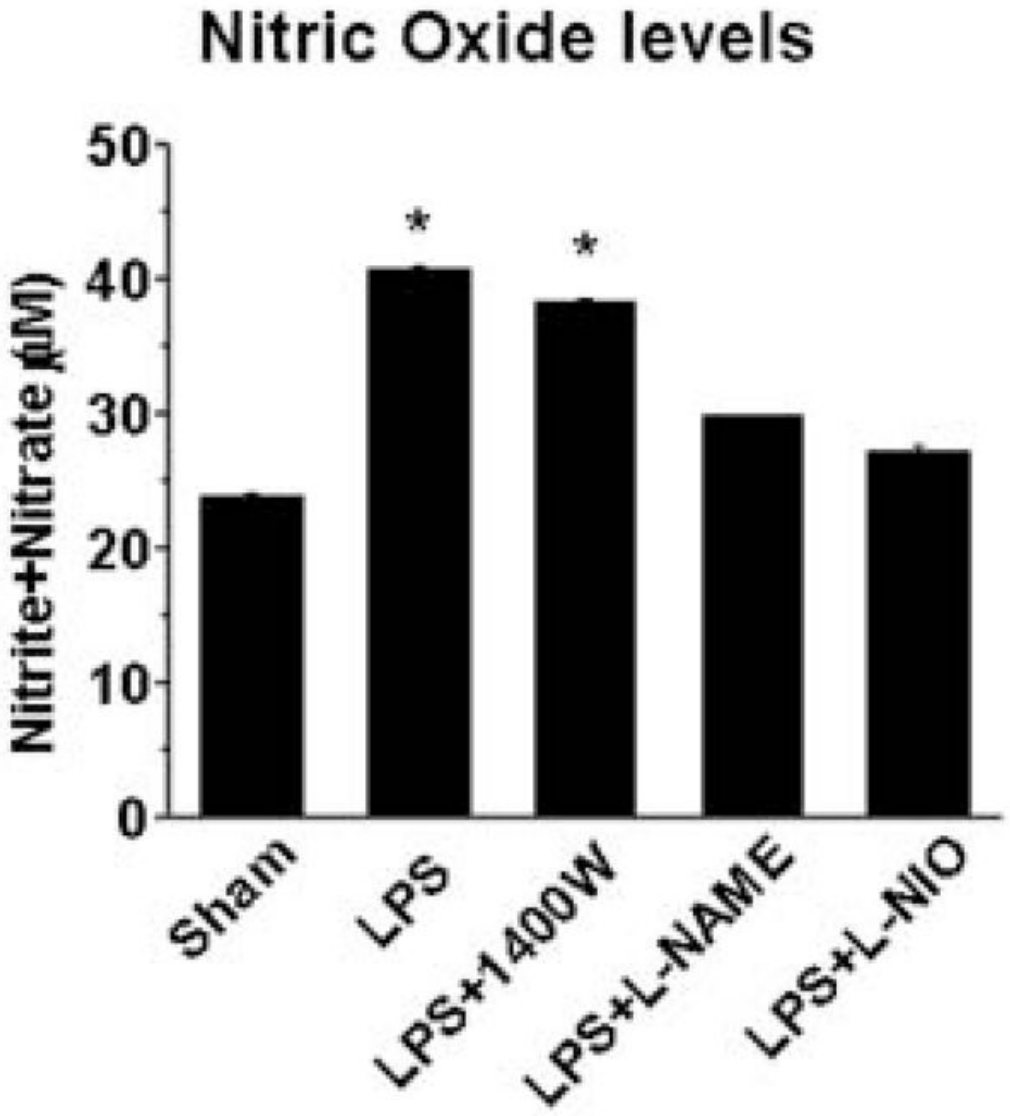

Fig. 7. Nitric oxide levels

Nitric oxide levels in spleen tissue homogenates from mice treated as shown were measured as the total nitrite plus nitrate. Data shown are the mean ±SE, with values significantly different ($P<0.05$) from the sham group indicated by an asterisk (*).

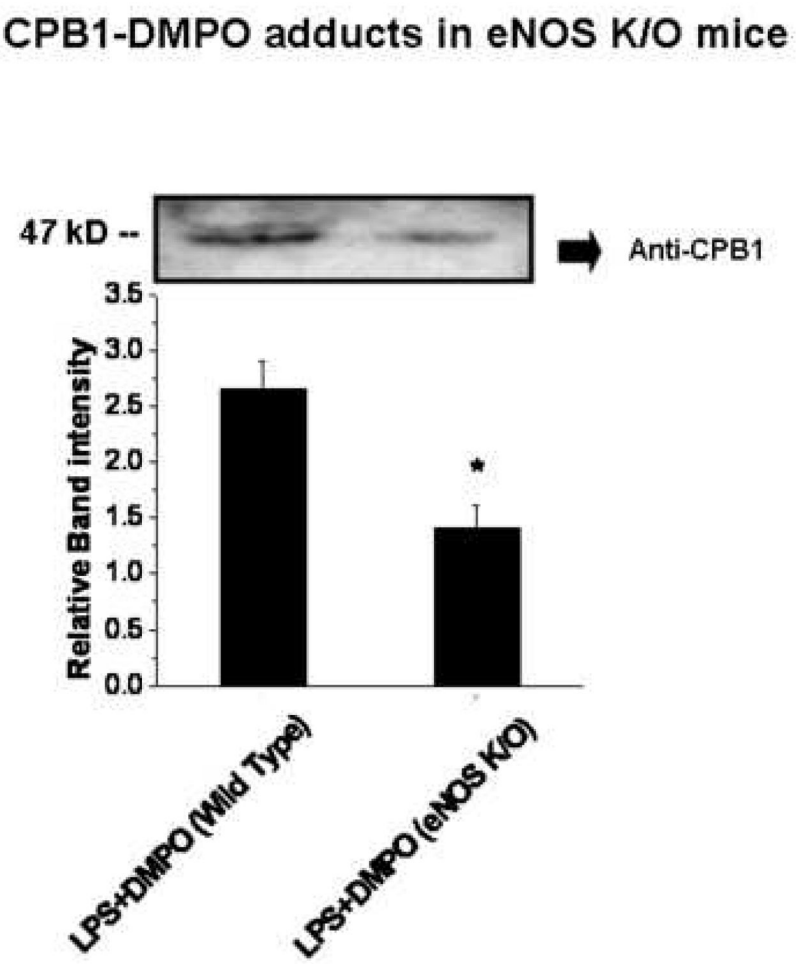

Fig. 8. CPB1-DMPO adducts in eNOS knockout mice

Protein from spleen tissue homogenates from wild-type and eNOS knockout mice were immunoprecipitated using anti-DMPO and were analyzed by Western blotting using anti-CPB1 (top panel). The Western blot represents results from 3 independent experiments with the best figure being displayed. Relative band intensities are shown in the bottom panel. Values represent the mean ± SE, with values significantly different ($P<0.05$) from the wild-type sample indicated by an asterisk (*).

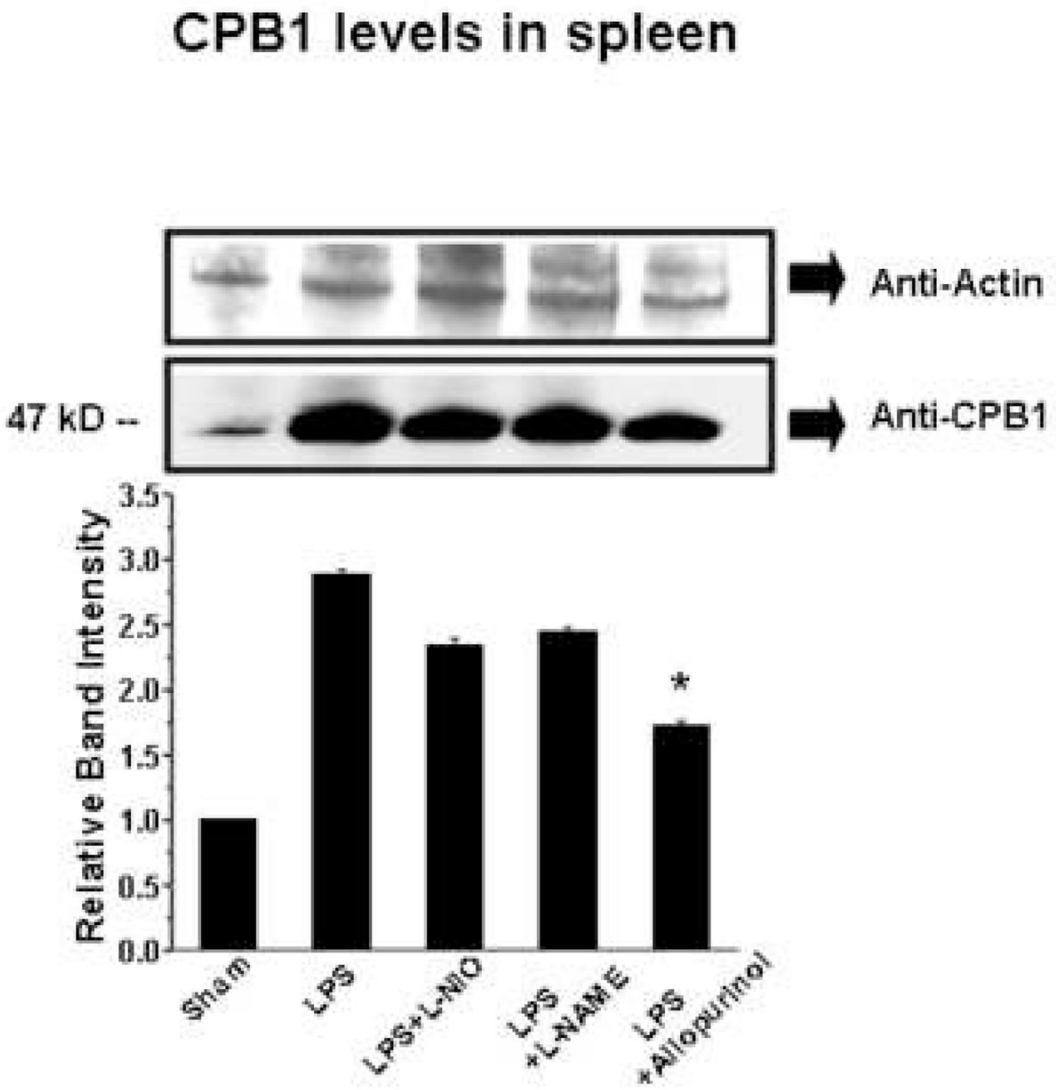

Fig. 9. Effect of NOS and xanthine oxidase inhibitors on CPB1 levels

Protein from spleen tissue homogenates from mice treated as shown were analyzed by Western blotting using anti-actin (top panel) as a loading control and anti-CPB1 (middle panel). The bottom panel shows the relative band intensity of the data in the anti-CPB1 Western blot. Values represent the mean ± SE, with values significantly different ($P<0.05$) from the LPS sample indicated by an asterisk (*).

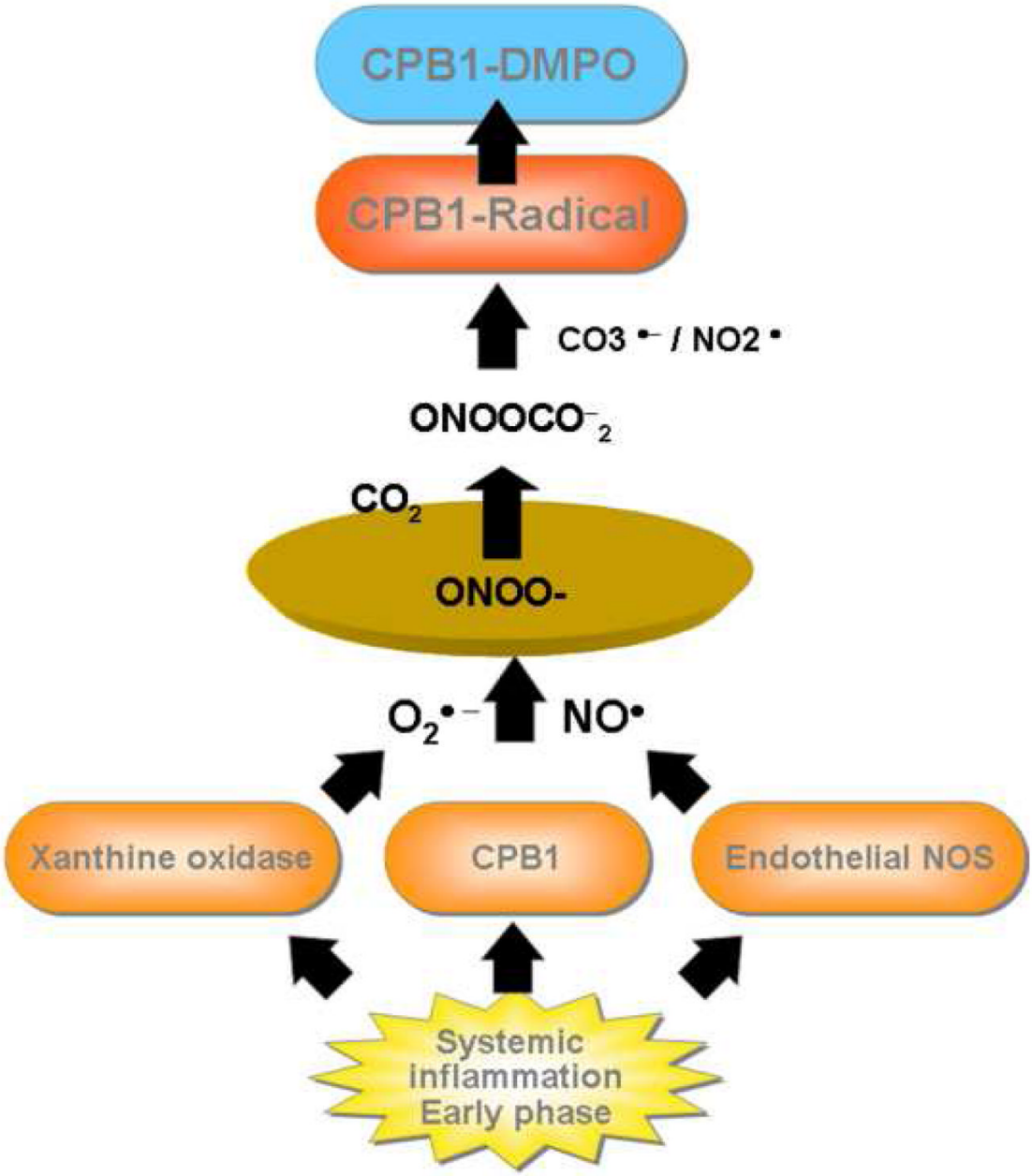

Scheme 1. Mechanism of formation of CPB1 radical in LPS induced systemic inflammation

Table 1

LC/MS/MS Protein Identifications[1] from Coomasie Blue Stained Gel Band which Corresponds to the anti-DMPO Positive Band in Mouse Spleen Homogenate

Protein	Number of Unique Peptides[2]	Protein Score[3]	Percent Sequence Coverage	Accession Number[4]	Entry Name
1	8	117.37	23	20864725	carboxypeptidase B1 (tissue)
2	2	38.03	4	29244176	keratin complex 2, basic, gene 1
3	1	22	8	16716569	trypsinogen 16

[1] Identifications were manually validated

[2] Number of unique tryptic peptides observed by LC/MS/MS

[3] Score based on Spectrum Mill scoring algorithm

[4] Accession number is the gi number from a search of the NCBI nonredundant database limited to mouse species only